Chinese Science Bulletin

© 2009 SCIENCE IN CHINA PRESS
Springer

Structure of aqueous sodium sulfate solutions derived from X-ray diffraction

XU JiXiang[1,2], FANG Yan[1†] & FANG ChunHui[1†]

[1] Key Laboratory of Salt Lake Resources and Chemistry, Qinghai Institute of Salt Lakes, Chinese Academy of Sciences, Xining 810008, China;
[2] Graduate University of Chinese Academy of Science, Beijing 100049, China

A rapid liquid X-ray diffractometer was used to study the time-averaged and space-averaged structure of aqueous sodium sulfate solutions at 298 and 323 K. Difference radial distribution functions of the solutions were obtained from accurate diffraction data. The interaction distances of Na^+-OH_2 and S-H_2O in solutions were found to be 0.235 and 0.385 nm, respectively, after deconvolution of superposition peaks by Gaussian multi-peak fitting program. The characteristic distance of the $NaSO_4^-$ contact ion pairs in higher concentration solutions was determined to be 0.345 nm, suggesting that the Na^+ ions coordinated with SO_4^{2-} ions in the mono-dentate form. Effects of concentration and temperature on the hydration structure of the solutions were discussed in the present paper. With a decrease in concentration, the contributions of the H_2O to the diffraction pattern increase, the average coordination number of the Na^+ ions hardly changes, while the hydration number of SO_4^{2-} ions increases slightly. The formation of $NaSO_4^-$ contact ion pairs becomes easier at higher temperature. The structure of hydrogen bond in dilute solutions is broken to a considerable extent with rising temperature, and the peak at 0.290 nm splits into two peaks at 0.275 and 0.305 nm, respectively.

solution structure, sodium sulfate, radial distribution function, contact ion pairs, X-ray diffraction

Aqueous solution of sodium sulfate exists extensively in the world. The hydration of sodium sulfate solution is decisive with regard to the progress and orientation of geochemical and chemical process in seawater, saline lake and underground brine. Since Na^+ may act as an essential element in enzyme catalysis processes, investigation of the solvation structure around hydrated Na^+ ions is crucial for understanding those processes. Sulfate particles, which are a well-known cause of adverse health effects and play a negative role in global climate[1], scatter incoming solar radiation and thus alter the nature of cloud, so detailed study of the hydration structure and property of SO_4^{2-} ions can help select better absorbents for sulfur dioxide control in acid rain.

At present, a number of studies have greatly paid attention to the structure of hydrated Na^+[2–5], while there has been no much literature focusing on the SO_4^{2-} hydration structure in aqueous solution. The hydrated sulfate ion in aqueous solution in structural and dynamic aspects using *ab initio* calculations and large angle X-ray scattering were studied by Vchirawongkwin et al.[6] The spectra of five low-energy $[SO_4(H_2O)_6]^{2-}$ structures with Gaussian 03 was computed and the gaseous $[SO_4(H_2O)_6]^{2-}$ structure formed by electrospray ionization (ESI) technology was discussed by Bush et al.[7] Based on photoelectron spectra of $SO_4^{2-}(H_2O)_n$, where n = 4 to 40, gaseous hydrated clusters of sulfate have been studied by Wang et al.[8] The results of X-ray dif-

Received November 15, 2008; accepted February 18, 2009
doi: 10.1007/s11434-009-0232-1
†Corresponding author (email: fangy8@isl.ac.cn, fangch@isl.ac.cn)
Supported by the National Natural Science Foundation of China (Grant No. 20873172) and Prior Special Fund of the Major State Basic Research Development of China (Grant No. 2008CB617612)

Citation: Xu J X, Fang Y, Fang C H. Structure of aqueous sodium sulfate solutions derived from X-ray diffraction. Chinese Sci Bull, 2009, 54: 2022-2027, doi: 10.1007/s11434-009-0232-1

fraction study of aqueous Na_2SO_4 solution with water-salt molar ratio of 1∶100 in the range of low scattering vector were reported by Смирнов et al.[9] However, the structural information on the effects of temperature and concentration on the hydration structures of Na_2SO_4 is still uncertain up to now. Based on these consideration above, a rapid liquid X-ray diffraction experiment in the range of large scattering vector on the $Na_2SO_4{\cdot}RH_2O$ solutions with R = 20 and 125 at 298 K and 323 K and the temperature and concentration dependence of aqueous structure will be reported in the present paper.

1 Experimental

(i) Samples preparation and analysis. Commercially available Na_2SO_4 (AR) was further recrystallized. Deionized water was redistilled twice in a quartz distilling apparatus. The concentrations of the samples were determined by gravimetry of barium sulfate. Densities of the solutions were calculated by using the empirical equation[10]. The compositions c, molar ratio R, density d, temperature T, linear absorption coefficient μ, stoichiometric volume V of the sample solutions are listed in Table 1.

Table 1 Physical properties of Na_2SO_4 solutions studied

Sample	c (mol·L^{-1})	R	d (g·cm^{-3})	T (K)	μ (cm^{-1})	V (nm^3)
A	2.576	20	1.294	298	2.429	0.322
B	2.547	20	1.279	323	2.401	0.326
C	0.440	125	1.053	298	1.351	1.885
D	0.436	125	1.043	323	1.338	1.904

(ii) X-ray diffraction measurements. X-ray diffraction was made on an X'Pert Pro θ-θ diffractometer by using Mo Kα radiation (λ = 0.07107 nm) of a second-generation ceramic Mo anode operated at 50 kV and 45 mA, as shown in Figure 1. A Zr filter installed in the diffracted beam was used to filtrate Mo Kβ radiation. The diffracted radiation was collected with an X'celerator detector[11]. The liquid sample cell with thermostat, designed by ourselves, was mounted on an infrared remote control positioning stage with motorized z-axial, tilt and φ movements. Four slits combinations, with 1/8, 1/4, 1/2 and 1° DS-ASS$_X$ slits for X'celerator detector, were employed for different 2θ regions. The sample solutions were scanned continually at different fixed time (400—4000 s). Accumulative count was greater than 1×10^4—5×10^4, and the statistical counting error was less than 1%. The diffraction angle range of measurements spanned over $3°\leqslant 2\theta \leqslant 150°$, corresponding to a range of 4.63 nm$^{-1}\leqslant s \leqslant$170.8 nm^{-1} of the scattering vector s ($s = 4\pi\sin\theta/\lambda$). In the case of the 1/4°DS-ASS$_X$ silt pair, the experiments were performed by free surface diffraction geometry. Because of the dry climate of Qinghai-Tibetan Plateau, the samples were covered by a Mylar foil of 6 μm in order to prevent composition change from evaporation of the solutions. Furthermore, Mylar's absorption intensity, as inferred from our experimental and calculated results, can be directly subtracted from total diffraction intensity. The goniometer must be aligned in the standard procedures for every diffraction measurement.

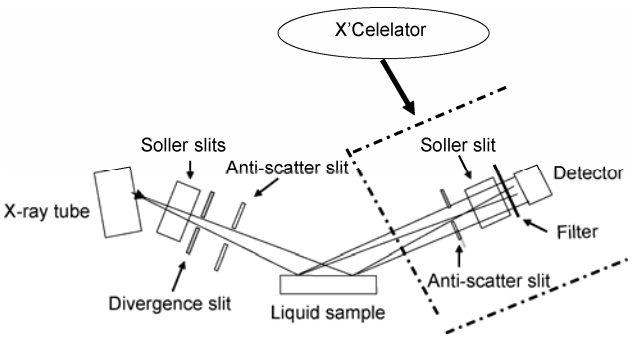

Figure 1 Geometric arrangement of the θ-θ diffractometer.

2 Data treatment

The intensity of four DS-ASS$_X$ slit pairs was converted to the intensity measured with the 1/2° silt pair from the data of overlapping regions after correction for background and absorption. Next, data smoothing, polarization, multiple scattering and geometric corrections of the converted intensity were performed. Finally, the corrected intensity was normalized to electron units by Krogh-Moe and Norman integration methods combined with high angle method.

The experimental structural function is defined as

$$i(s) = K{\cdot}I_p(s) - \sum_{i=1}^{N_{atom}} x_i\,[f_i^2(s)+(\Delta f_i'')^2+\mathrm{del}(s){\cdot}I_i^{incoh}(s)], \quad (1)$$

where s is scattering vector, and K is scaling coefficient. $I_p(s)$ represents the intensity of polarization correction, and $K{\cdot}I_p(s)$ is the scaling intensity in electron units. N_{atom} is the number of atoms in the solution. x_i is the number of ith atom in the stoichiometric volume containing one Na atom. $f_i(s)$ is the atomic scattering factor corrected for the real parts of the anomalous dispersion, $f_i(s) = f_i + \Delta f_i'$.

$\Delta f_i'$ and $\Delta f_i''$ are the real and the imaginary parts of the anomalous dispersion correction, respectively. The coherent scattering factors f_i of spherical free atom and its correction term were taken from the International Tables for X-ray Crystallography[12]. del(s) is the fraction of the incoherent radiation reaching the counter. Because the monochromator was not equipped in the diffracted beam, the value of del(s) is 1. $I_i^{\text{incoh}}(s)$ is Compton scattering of atom i, its value was taken from the literature[12] and multiplied by Breit-Dirac recoil factor.

The difference radial distribution function (DRDF) was computed from s-weighted structure function $s \cdot i(s)$ by the Fourier transformation, according to eq. (2)

$$D(r) = 4\pi r^2\rho_0 + (2r/\pi)\int_0^{s_{\max}} s \cdot i(s) \cdot M(s) \cdot \sin(sr)\mathrm{d}s\,, \quad (2)$$

where r is the interatomic distance, ρ_0 is the average electronic diffracting power at zero angle of the sample ($e^2 \cdot nm^{-3}$). $M(s)$ is the modification function[1)]. To remove spurious peaks at small r values in the DRDF curve, a Fourier transformation procedure was reused to correct the experimental structure function.

The theoretical structural function calculated on the basis of a geometric model is obtained by

$$i_{\text{calcd}}(s) = \Sigma\,\Sigma x_i n_{ij} f_i f_j \frac{\sin(sr_{ij})}{sr_{ij}} \exp(-b_{ij}s^2). \quad (3)$$

Equation (3) is related to the short-range interactions characterized by the interatomic distance r_{ij}, the temperature factor b_{ij} and the number of interactions n_{ij} for each atom pair i-j. In this work, the long-range interactions between a spherical hole and the continum distance distribution were not considered in detail. All the data were analyzed by means of the Origin software and KURVLR 2005 for SR program[1)].

3 Results and discussion

3.1 Structure functions

Experimental structural functions $i(s)$, which represent the extent of interference between atoms i and j, contain a lot of structural information. The s-weighted structural functions $s \cdot i(s)$ are presented in Figure 2(a). The $s \cdot i(s)$ curves remain oscillated near the zero axis, showing that the diffraction experiments and data treatment processes are reliable.

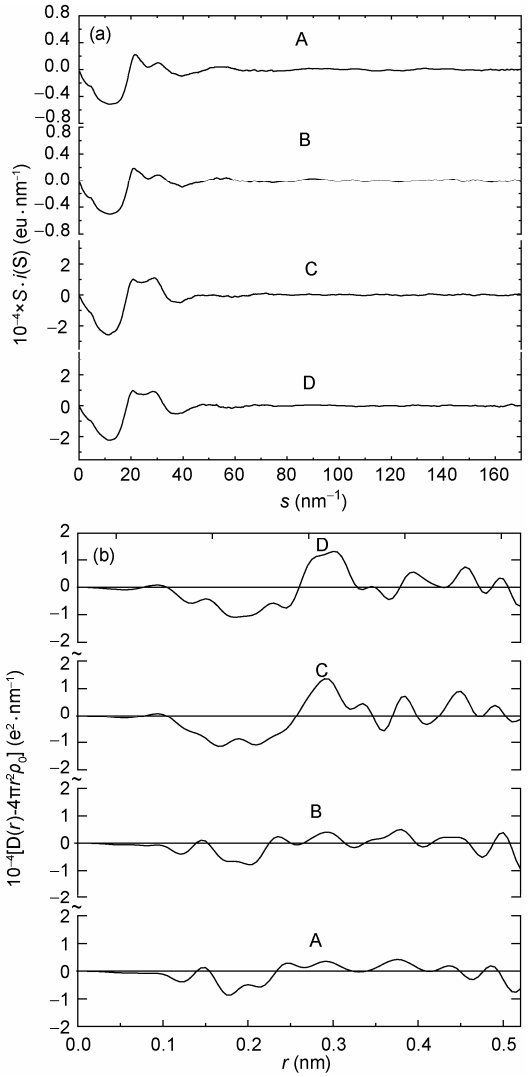

Figure 2 S-weighted structure functions (a) and DRDFs (b) for Na_2SO_4 solutions.

3.2 Radial distribution functions

Figure 2(b) shows the DRDF in the form of $D(r) - 4\pi r^2\rho_0$ for the sample solutions investigated. There are no spurious peaks within 0.1 nm in the curve DRDF– r. Therefore, it may be concluded that statistical and systematic errors are reduced to the minimum.

(1) Overlapping peaks treatment. As seen in Figure 2(b), the peaks in the range of 0.200—0.300 nm for the dilute solutions C and D are so broad that they could be formed from several different interactions. In order to accurately describe the atomic arrangement in the solution, the extent of static disorder for hydrated structure

1) Fang C H, Fang Y, Wang L Y. Handbook of Solution Structure of X-ray Data Analyzing Program KURVLR and Structure Parameter Refinement Program PUTLSQ (in Chinese). Xining: Science-Technology Documentation of Institute of Salt Lakes, Chinese Academy of Science, 1997. 186

and the coordination number between the nearest atoms in aqueous solutions, the Gaussian Multi-peaks fitting program is employed to deconvolve the overlapping peaks.

The typical results of the peak fitting procedure on the DRDF curves for the solutions C and D are shown in Figure 3. The overlapping peaks and experimental peaks approximately coincide. Therefore, six Gaussian components contribute to the observed DRDFs over the r range analyzed. The interatomic distances of all separation peaks are listed in Table 2.

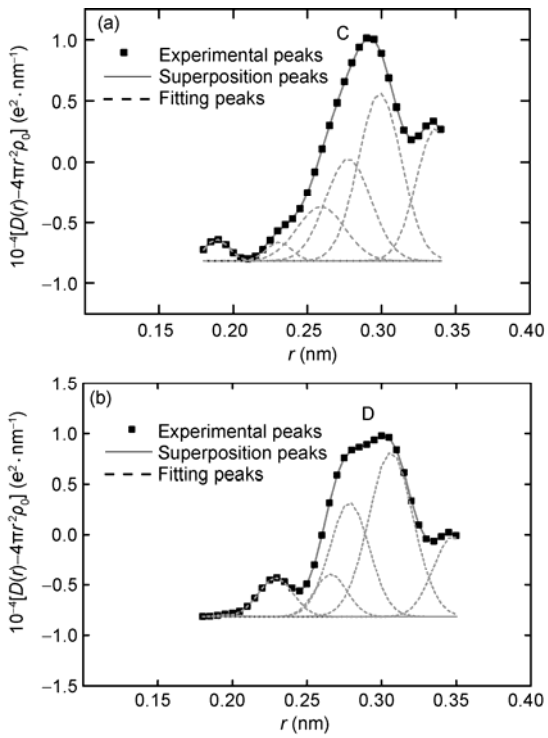

Figure 3 Multi-peaks fitting curves of $Na_2SO_4 \cdot 125H_2O$ samples at 298 K (a) and 323 K (b).

Table 2 The fitting peaks position obtained for solutions of samples C and D (nm)

Sample	Peak					
	1	2	3	4	5	6
C	0.189	0.231	0.259	0.278	0.299	0.337
D	0.197	0.229	0.266	0.278	0.306	0.347

(2) Interactions determination. According to the crystal structure data of Na_2SO_4[13] and $Na_2SO_4 \cdot 10H_2O$[14] reported in the literature and pervious findings in X-ray diffraction experiments of Na^+, SO_4^{2-} and liquid water, interaction pair of every peak is determined after obtaining the DRDFs of four solutions.

The first peak of about 0.095 nm can be assigned to intramolecular O—H interactions in H_2O molecules. The peak at 0.153 nm is S—O_S nearest-neighbor distance within sulfate ion, and this assignment is suggested by the crystal structure data of Na_2SO_4[13] and $Na_2SO_4 \cdot 10H_2O$[14]. Since the distance 0.250 nm is close to a tetrahedral edge length ($\sqrt{8/3} \cdot 0.153 = 0.250$ nm), the peak at 0.250 nm can be ascribed to O_S—O_S interactions in sulfate group. The first hydration shell distance of Na^+ in investigated solutions is 0.235 nm, which agrees with the previous findings[15], and the Na^+-OH_2 second sphere is observed at 0.441—0.480 nm. The coordination number of Na^+ is 6 for the first hydration shell and 8—12 for the second hydration shell, respectively. The interactions between coordinated SO_4^{2-} ions and water molecules hydrogen-bonding to the sulfate ions, which usually appear at 0.370—0.393 nm as found in aqueous sulfate solution[15], contribute to the peak at about 0.385 nm, and the solvation shell of SO_4^{2-} ion is composed of seven to twelve water molecules. As for pure water structure, the research results reported three peaks at around 0.095, 0.185 and 0.330 nm for O—H interactions, and three peaks at about 0.283, 0.444, and 0.660 nm for O—O interactions[16]. Because the X-ray scattering power of the H atoms is too low for detection with reliable accuracy, the H—H interactions are not discussed in these experiments. Therefore, all the O—H and O—O peaks will occur at corresponding positions on the DRDF curves of aqueous Na_2SO_4 solutions. In Figure 2(b), a peak is observable around 0.332 nm, close to an octahedral edge length $\sqrt{2} \cdot r_{Na^+\text{-}OH_2}$, which can be assigned to *cis*-H_2O-H_2O interactions around Na^+. In Table 2, a peak at 0.278 nm is close to O—O bond length of water-water. Because Na^+ acts as a 'structure-making' ion[17] which forms a rather strong hydrated complex, the peak at 0.278 nm is related to the hydrogen bonds between the water molecules in the first and second coordination shells of Na^+ ions.

At 0.345 nm, a peak is observable in concentrated solutions, which can be attributed to $NaSO_4^-$ contact ion pairs. This assumption is supported by the mean distance of Na—S (0.342 nm) in crystal structure of Na_2SO_4[13], thus it may be inferred that the electrostatic attraction between Na^+ and SO_4^{2-} ions is weakened in solutions. Furthermore, The Na^+—O—S angle is 127° calculated

by cosine theorem, indicating that Na^+ ions coordinated with SO_4^{2-} ions in the mono-dentate form. Wang et al.[18] have found evidence of the $NaSO_4^-$ contact ion pairs formation in the gas phase by means of photoelectron spectroscopy and density functional theory and *ab initio* molecular orbital theory. Extent of coupling between Na^+ ions and SO_4^{2-} ions was evaluated by Leaist et al.[19], showing that extent of association is larger than 0.45 in 2.25 mol/L solution. Those conclusions discussed above can further support our assumption.

3.3 Model fittings

The theoretical DRDFs of Na_2SO_4 sample solutions are gained by inputting the structural parameters(c, r_{ij}, n_{ij}, b_{ij}) obtained from the preliminary analysis above and previous studies of Na^+ and SO_4^{2-} ions in water. The structural parameters were allowed to vary until the patterns of experimental DRDFs were resembled to the theoretical ones. Next, the rough structural parameters were refined by means of NLPLSQ programs. Lastly, the refined structural parameters were inputted into KURVLR program again to verify its adaptability. This process was repeated alternately many times until the optimal parameters were obtained. The finally refined results will be discussed further elsewhere.

3.4 Concentration effects

The DRDFs of Na_2SO_4 solutions at different concentrations are shown in Figure 4. By the decrease of concentration, the O—H and O—O peaks increase due to the increased content of water in the aqueous solutions, whereas the peaks at 0.150 nm S—O_S and 0.250 nm O_S—O_S decrease, which can be explained by the decreased concentration of S—O_S and O_S—O_S-type contributions to the diffraction pattern. As can be seen in Figure 4, the O—O distance shifts to a large r value with increasing concentration at room temperature, indicating that the O—O interactions between water molecules in the bulk water gradually decrease and the contact ion pairs appear at higher concentration[20]. With a decrease in concentration, a rather complex and broad main peak can be seen at about 0.290 nm at 323 K, which splits into two asymmetric peaks at about 0.275 and 0.305 nm, suggesting that more than one interactions give rise to this peak. The peak at about 0.340 nm decreases with increasing concentration, the reason for this change is probably that the partial water molecules in the first hydration shell of sodium ions are replaced by SO_4^{2-} ions, forming the $NaSO_4^-$ contact ion pairs. As a result, the peak arising from the *cis*-H_2O—H_2O interaction within Na^+ complexes tends to diminish. With decreasing solute concentration, the positions of the peaks at 0.380 and 0.440 nm respectively shift to a slightly larger r value. These results show that water molecules bound to SO_4^{2-} and Na^+ ions increase, and the SO_4^{2-}—H_2O_I and Na^+—H_2O_{II} distances become greater.

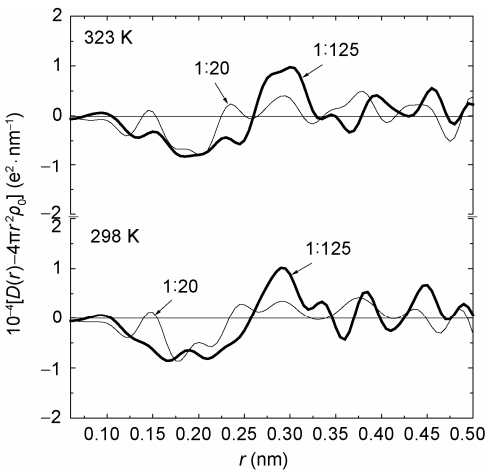

Figure 4 Comparison of DRDFs for aqueous Na_2SO_4 solutions at different concentrations.

3.5 Temperature effects

Figure 5 shows the DRDFs of Na_2SO_4 solutions at different temperatures. The hydration structures of ions are rather sensitive to temperature change. In dilute solutions, the peak assigned to S—O_S interactions increases, while it hardly varies in concentrated ones. Around 0.19 nm, a peak can be found, which can be attributed to intermolecular H—O interactions between water molecules. This peak deceases with increasing temperature, which explained the increase of extent of the break or the bend of the hydrogen bond in the bulk water. With an increase in temperature, the peak of Na^+—OH_2 becomes sharper, and the position of this peak shifts to a small r value. Moreover, the O_S—O_S interactions at 0.250 nm diminish, suggesting that the pattern of SO_4^{2-} group may be deformed at higher temperature. As shown in the inset of the Figure, the peak at 0.290 nm in dilute solutions splits into two peaks at higher concentration, indicating that the O—O interactions are also sensitive to temperature variation. The peak at 0.345 nm in concentrated solutions becomes shaper with increasing temperature, showing that higher temperature is in favor of

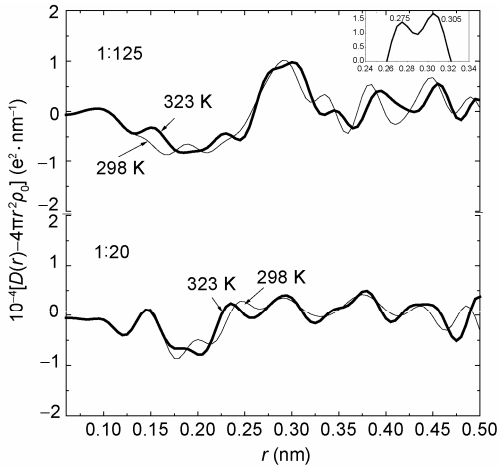

Figure 5 Comparison of DRDFs for aqueous Na_2SO_4 solutions at different temperatures.

forming contact ion pairs. This result is in good agreement with the conclusions drawn by Leaist[19] and the phase diagram of Na_2SO_4-H_2O system[21]. On the contrary, the peak at 0.345 nm in concentrated solutions becomes flatter with increasing temperature.

4 Conclusions

X-ray diffraction experiments of aqueous Na_2SO_4 solutions with different concentrations and temperatures were performed. The hydration structure of Na^+ ions is rather sensitive to changes of concentration and temperature, and the average coordination number of the Na^+ is almost constant. The coordination number and interaction distance of hydrated SO_4^{2-} ions increase with decreasing concentration. With an increase in concentration and temperature, the network structure of water in the bulk water is broken to a considerable extent, and the H_2O-H_2O interaction centered around 0.290 nm splits into two peaks at 0.275 and 0.305 nm, respectively. The formation of $NaSO_4^-$ contact ion pairs with a bond length of 0.345 nm was verified from the measurements of the more concentrated Na_2SO_4 solutions, and higher temperature and concentration in favor of forming contact ion pairs are suggested.

1 Laskin A, Gaspar D J, Wang W H, et al. Reactions at interfaces as a source of sulfate formation in sea-salt particles. Science, 2003, 301: 340－344 [DOI]
2 Ikeda T, Boero M, Terakura K. Hydration of alkali ions from first principles molecular dynamics revisited. J Chem Phys, 2007, 126: 1－9
3 Carrillo-Tripp M, Saint-Martin H, Ortega-Blake I. A comparative study of the hydration of Na^+ and K^+ with refined polarizable model potentials. J Chem Phys, 2003, 118: 7062－7073[DOI]
4 White J A, Schwegler E, Galli G, et al. The solvation of Na^+ in water: First-principles simulations. J Chem Phys, 2000, 113: 4668－4673[DOI]
5 Koneshan S, Rasaiah J C. Computer simulation studies of aqueous sodium chloride solutions at 298 K and 683 K. J Chem Phys, 2000, 113: 8125－8137[DOI]
6 Vchirawongkwin V, Rode B M, Persson I. Structure and dynamics of sulfate ion in aqueous solutions an *ab initio* QMCF MD simulation and large angle X-ray scattering study. J Phys Chem B, 2007, 111: 4150－4155[DOI]
7 Bush M F, Saykally R J, Williams E R. Evidence for water rings in the hexahydrated sulfate dianion from IR spectroscopy. J Am Chem Soc, 2007, 129: 2220－2221[DOI]
8 Wang X B, Yang X, Nicholas J B, et al. Bulk-Like features in the photoemission spectra of hydrated doubly charged anion clusters. Science, 2001, 294: 1322－1325 [DOI]
9 Смирнов П Р, Тростин В Н, Крестов Г А. Д-структуры водных растворов сульфатов металлов из дифракционных данных. Ж Физ Хим, 1988, 62: 925－928
10 Fang C H. A new theoretical model of prediction salt lake brine density (in Chinese). J Salt Lake Res, 1990, 15－20
11 Fukuda K, Iwata T, Nishiyuki K. Crystal structure, structural disorder, and hydration behavior of calcium zirconium aluminate, $Ca_7ZrA_{l6}O_{18}$. Chem Mater, 2007, 19: 3726－3731[DOI]
12 Prince E. International Tables for Crystallography. 3rd ed. London: Kluwerr Acad Pub, 2004
13 Naruse H, Tanaka K, Morikawa H, et al. Structure of Na_2SO_4 (I) at 693K. Acta Cryst, 1987, B43: 143－146
14 Levy H A, Lisensky G C. Crystal structures of sodium sulfate decahydrate (Glauber's Salt) and sodium tetraborate decahydrate (Borax). redetermination by neutron diffraction. Acta Cryst, 1978, B34: 3502－3510
15 Ohtaki H, Radnai T. Structure and dynamics of hydrated ions. Chem Rev, 1993, 1003: 1157－1204[DOI]
16 Head-Gordon T, Hura G. Water structure from scattering experiments and simulation. Chem Rev, 2002, 102: 2651－2670[DOI]
17 Tongraara A, Rode B M. Dynamical properties of water molecules in the hydration shells of Na^+ and K^+: *Ab initio* QM/MM molecular dynamics simulations. Chem Phys Lett, 2004, 385: 378－383[DOI]
18 Wang X B, Ding C F, Nicholas J B, et al. Investigation of free singly and doubly charged alkali metal sulfate ion pairs: $M^+(SO_4^{2-})$ and $[M^+(SO_4^{2-})]_2$ (M = Na, K). J Phys Chem A, 1999, 103: 3423－3429[DOI]
19 Leaist D G, Goldik J. Diffusion and ion association in concentrated solutions of aqueous lithium, sodium, and potassium sulfates. J Solution Chem, 2001, 30: 103－118[DOI]
20 Megyes T, Grósz T, Radnai T, et al. Solvation of calcium ion in polar solvents: An X-ray diffraction and *ab initio* study. J Phys Chem A, 2004, 108: 7261－7271[DOI]
21 Здановский А В, Соловьева Е Ф, Эзрохи Л Л. Справочник по растворимости солевых систем том третий. Ленинград: Государственное научно-техническое издательство химической литературы, 1961. 1639－1640